20th Australasian Fluid Mechanics Conference
Perth, Australia
5-8 December 2016

Internal Tide Breaking at Topography

S. Legg[1]

[1]Atmospheric and Oceanic Sciences Program
Princeton University, Princeton, NJ 08540, USA

Abstract

Breaking internal waves drive much of the mixing in the stably stratified ocean interior. Tidal flow over topography is one source for generation of these internal waves. Numerical simulations reveal several mechanisms for breaking of internal tides, including transient hydraulic jumps, nonlinear wave-wave interactions and wave reflection from sloping and shoaling topography. In all three scenarios, the steepness of the topography has a strong influence on the wave-breaking behavior. Quantification of the net loss of energy from the internal waves to small-scale motion and dissipation, and the dependence of that dissipation on topographic parameters, stratification and flow amplitude provides guidance for parameterizations of internal-tide driven mixing suitable for climate models. Coupled climate model simulations demonstrate the impact of the distribution of internal-wave driven mixing on the large-scale circulation and climate.

Introduction

Mixing in the stably stratified ocean interior is largely driven by breaking internal waves. While the mixing is an important component of the large-scale ocean circulation, the coarse resolution global ocean models used for climate prediction cannot simulate either the mixing or the generation and propagation of the internal waves that lead to the mixing. An energetically consistent parameterization of ocean mixing for climate models must therefore represent the transfer of energy to the internal waves, the propagation of that energy, and the ultimate loss of the wave energy to mixing when waves break. A major source of internal wave energy comes from the barotropic tide, which generates internal tides through flow over topography in a stratified fluid. Significant progress has been made in predicting the conversion of energy from the barotropic tide to internal waves, as a function of the tidal flow, topographic parameters and buoyancy stratification [7]. A commonly used parameterization [26] builds on predictions of this energy conversion to represent the tracer diffusivity κ due to breaking internal tides as follows:

$$\kappa = \frac{\Gamma \varepsilon}{N^2} \; ; \varepsilon = \frac{1}{\rho} E(x,y) q F(z) \tag{1}$$

where Γ is the mixing efficiency, $N^2 = -g/\rho_0 d\rho/dz$ is the squared buoyancy frequency, ε is the kinetic energy dissipation, ρ is the density, $E(x,y)$ is the energy conversion from barotropic to baroclinic tide, q is the fraction of converted energy which is used for local dissipation at the generation site and $F(z)$ is the vertical distribution of that dissipation. In standard implementations of this parameterization [24], q, the fraction of energy dissipated locally, is assumed to be a constant (typically 30%) and $F(z)$ describes an exponential decay away from the bottom, with a fixed decay scale. The remainder of the internal tide energy is assumed to propagate away from the generation site and ultimately lead to a constant background diffusivity. The choice of fixed local fraction of dissipation, exponential decay with fixed decay scale, and constant background diffusivity, all ignore the details of the physics of the internal wave breaking processes.

Here we explore refinements to this approach, using numerical simulations motivated by recent observations to explore the physical processes of internal wave breaking. In particular, we examine the factors that influence the fraction of internal tide energy which is dissipated locally q, and different vertical profiles of dissipation $F(z)$ which result from different wave-breaking processes. Some of the processes leading to far-field breaking of the propagating internal waves are also explored, allowing a spatially variable far-field dissipation model to be developed.

Internal wave breaking is often characterized by a nonlinear steepening of the wave, associated with Froude number $Fr \geq 1$ where

$$Fr = \frac{U}{C_p}. \tag{2}$$

U is the flow speed, and C_p is the horizontal phase speed. Internal waves have horizontal phase speeds that scale like $C_p \approx N/m$, where m is the vertical wavenumber. Smaller wavelength waves therefore have slower phase speeds, and are more likely to have large Fr. Scenarios which lead to internal wave breaking are often those which increase Froude number, either by increasing the flow speed or by reducing the wavelength of the internal waves.

The interaction between internal waves and topography is sensitive to the steepness of the topography where the relevant nondimensional measure of topographic steepness is

$$\gamma = \frac{|\nabla h|}{s} \; ; s = \sqrt{\frac{\omega^2 - f^2}{N^2 - \omega^2}} \tag{3}$$

where s is the slope of the internal wave group velocity vector, where f is the coriolis parameter, ω is the wave frequency, and N is the buoyancy frequency. Steep "supercritical" topography has $\gamma > 1$, shallow "subcritical" topography has $\gamma < 1$, and critical slope topography has $\gamma = 1$.

Methods

Numerical simulations are carried out using the MITgcm, forced by either the barotropic tide (imposed as an oscillating body force) or by a internal wave at the tidal frequency with a mode-1 vertical structure propagating in from the boundary. Many of the simulations described here are two-dimensional, in the vertical and one horizontal direction, but some, involving more complex topography, are 3 dimensional. The fluid is initially stably stratified, and rotating and nonhydrostatic dynamics are employed.

Local Dissipation

As the barotropic tide flows over submarine topography, exciting internal waves, some wave breaking takes place near the generation site, leading to local dissipation. The processes leading to dissipation vary depending on the height and steepness of the topography.

Tall Steep Topography

At tall steep topography, numerical simulations show overturning associated with transient internal hydraulic jumps downslope from the topographic peak [16], consistent with observations from tall steep ridges such as the Hawaiian ridge [13] and the Luzon Straits [1]. These internal hydraulic jumps only occur if the topography is both tall enough to block the flow ($Nh/U > 1$) and steep enough that tidal vertical excursions are large enough that this blocking effect is realized during the tidal cycle ($\gamma \geq 2$).

An estimate of the energy lost to dissipation and mixing in these overturning features can be made by assuming that internal hydraulic jumps occur when $U_{bt} > [C_p]_n$, where U_{bt} is the barotropic flow speed and $[C_p]_n$ is the phase speed of mode n, such that internal wave mode n is arrested by the barotropic flow [12]. This assumption leads to a dissipation estimate which scales like U^3, as observed in the Hawaiian ridge region. The dissipation is concentrated near the topography with a vertical lengthscale which scales like U/N. This theoretical estimate for the local dissipation agrees well with numerical simulations of 2D steep ridge topography. The fraction of total internal tide energy which is dissipated through these arrested waves is however small, typically around 20%, and the remainder of the internal wave energy propagates away from the generation site in the form of low-mode internal tides.

When the barotropic tide flows over adjacent ridges, interference between the ridges can lead to enhancement or reduction in the net dissipation, depending on the relative height and spacing of the ridges. For the Luzon Straits, constructive interference during periods when the tide is largely semi-diurnal in frequency leads to local dissipation of about 40% of the internal tide [3].

Small-scale Rough Topography

At the smaller-scale rough topography typical of ocean spreading zones, such as the MidAtlantic Ridge, where bottom enhanced mixing has been observed [23], an internal tide field with a broad spectrum of wave-lengths propagates upward from the topography. Only the smallest wavelength topography is able to generate internal tides with small enough vertical wavelengths to lead to wave breaking [25]. For longer wavelengths nonlinear interactions between the internal tides can transfer energy to waves at lower frequencies with smaller vertical wavelengths where breaking is possible [21]. Nonlinear wave-wave interaction theory suggests that this process of energy transfer to smaller scales is enhanced at smaller wavelengths, and strongly dependent on Coriolis. In particular, resonant triad interactions are only possible if $f < \omega/2$, and at the critical latitude where $f = \omega/2$, the growth rate of this parametric subharmonic instability becomes very large. The impact on the wave breaking and subsequent energy dissipation is seen in the fraction of internal tide energy which is dissipated locally in numerical simulations: this ratio scales inversely with the topographic wavelength and reaches a peak at the critical latitude [28]. This scaling is however sensitive to the topographic steepness: for subcritical topography, $\gamma < 1$, all internal wave energy propagates upward, and wave-wave interactions and the sensitivity to coriolis dominate. For steep topography, $\gamma > 1$, much of the internal tide energy propagates downward into the topographic troughs, where large dissipation results from energy focusing with less dependence on wave-wave interaction and therefore less sensitivity to Coriolis, figure 1.

Away from the critical latitude, the vertical profile of dissipation is consistent with that suggested by wave-wave interaction theory [22], with an algebraic decline above the topography. However, at the critical latitude, there is a thick layer of near-uniform dissipation, corresponding to the region populated by near-inertial waves resulting from the instability, followed by a precipitous decline to background levels of dissipation higher in the water column [21].

Internal waves which continue to propagate up into the thermocline may transfer energy to smaller-scales as stratification increases, leading to an increase of dissipation with stratification [22]. Finally any remaining upward-propagating small scale internal tides can reflect from the base of the mixed layer or the ocean surface, and return to scatter from the topography at the ocean floor [2]. As a result of these different processes for small-scale internal wave dissipation in the water column and at the topography, little wave energy may propagate horizontally out of the region of rough topography.

Farfield Dissipation

The low-mode internal tides which do not break near their generation site can propagate long distances around the globe [29]. While several processes can lead to dissipation of these waves in the deep ocean basins (e.g. nonlinear wave-wave interaction [17], scattering from rough topography, interaction with mesoscale eddies [6]) our focus here is on the interaction of low-mode internal waves with large-amplitude topographic slopes such as the continental slope or large ridges. This interaction is strongly dependent on the relative steepness of the topographic slope [15], [14].

Steep Continental Slopes

When low-mode internal tides encounter steep topographic slopes, $\gamma >> 1$, most of the internal wave energy is reflected back to the deep ocean [10]. However, when the reflected signal contains higher mode components which have phase speeds slower than the fluid velocity at the top of the slope (which results from the superposition of incoming, reflected and transmitted waves) those waves may be arrested and break, similarly to waves generated at tall steep slopes. This breaking process is however inefficient, and results in a maximum loss of about 10% of the incoming wave energy [11]. Dissipation is concentrated near the top of the steep slope.

Critical and Subcritical Continental Slopes

Numerous studies have shown that when internal waves hit a slope which is at or near the critical slope, $\gamma \approx 1$, the reflected wave will have very high wavenumbers and energy density concentrated along the topographic slope, leading to a turbulent region along the slope [8] [9]. The net loss of energy from an incoming wave is then proportional to the fraction of the total depth occupied by the critical slope, WKB-scaled for variations in stratification, and independent of the Froude number of the incoming wave [14]. By contrast, for a subcritical slope, all the wave energy is transmitted towards shallower water, with little change in mode number. However, as the water depth shoals, energy becomes concentrated in less and less water, increasing the Froude number through a reduction in vertical wavelength combined with increase in wave flow amplitude. For large enough initial Froude number and significant changes in depth, the final Froude number can be sufficient to cause breaking [14].

The topographic steepness also influences the vertical distribution of the dissipation due to the breaking wave. Whereas at critical slopes, the dissipation is concentrated adjacent to the slope, at subcritical slopes, the overturning of the low-mode wave in shallow water distributes dissipation throughout the water column [14].

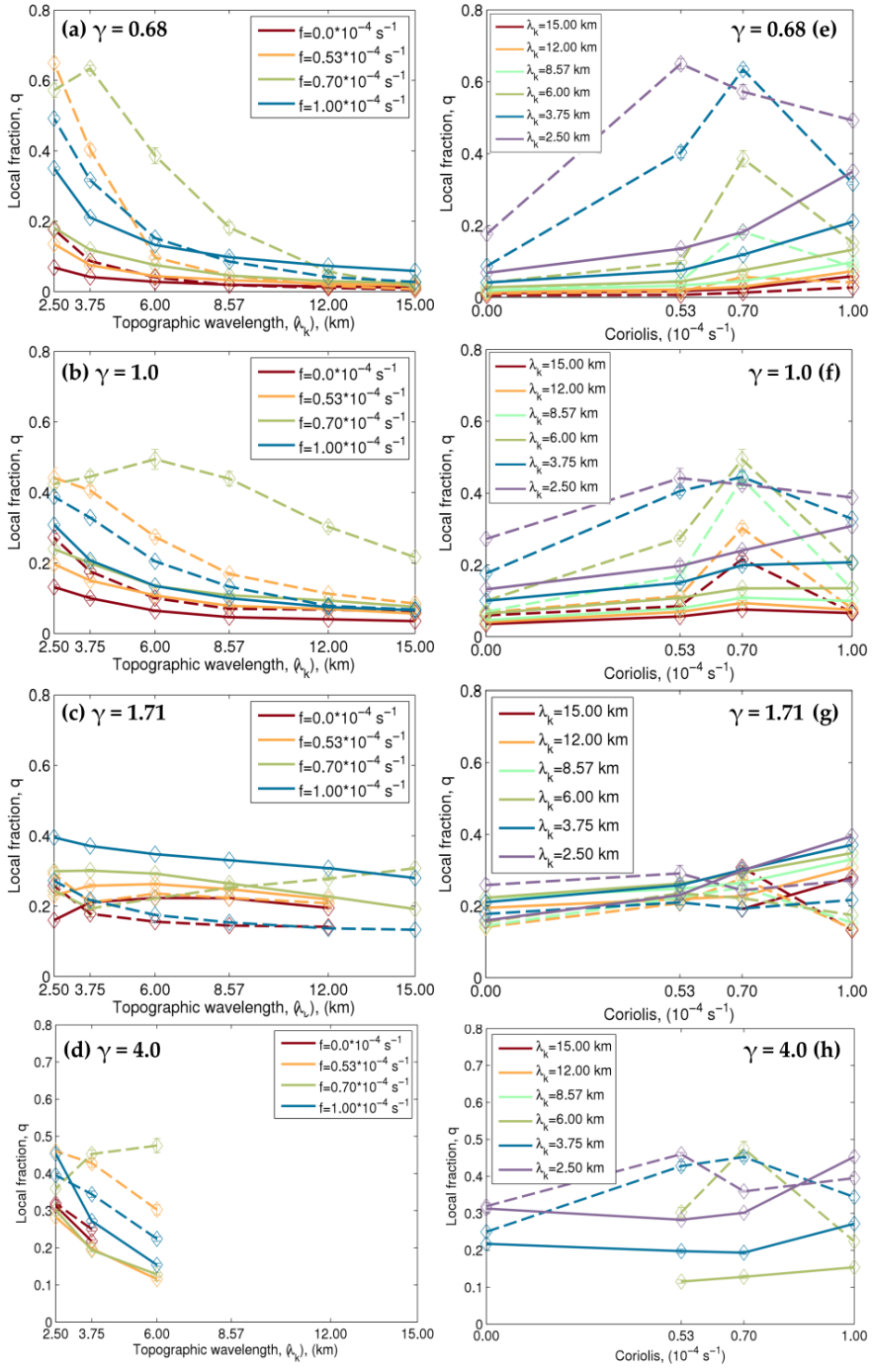

Figure 1: The fraction of energy dissipated locally q for internal waves generated by M2 tidal flow over sinusoidal topography, as a function of topographic wavelength λ_k (a-d), and coriolis f_0 (e-h), for four different topographic steepness γ. Solid lines show the fraction of energy dissipated below $50m$ above the bottom, while dotted lines show the fraction of energy dissipated from $50-2000m$ above bottom. For critical $\gamma = 1$ and subcritical $\gamma < 1$ topography, the local fraction of dissipation at $50-2000m$ above the bottom decreases with λ_k and peaks at the critical latitude $f_0 = 0.7 \times 10^{-4} s^{-1} = \omega/2$. For supercritical topography $\gamma > 1$, the dependence of local dissipation on both wavelength and coriolis is less marked. From [28]

Continental Slope Canyons

Real continental slopes are not infinite planar slopes, and the wave breaking process can be strongly influenced by variations in the slope in the along-slope direction. Canyon-like incisions are widespread along the continental slope [4]. Three-dimensional simulations of low-mode internal wave scattering from continental slope canyons show that wave breaking can be greatly enhanced by the three-dimensional geometry of the canyon [20]. In particular, whereas dissipation at steep continental slopes is small for uniform along-slope topography [11], when a V-shaped flat-bottomed canyon with steep side-walls is introduced into the continental slope, the incoming wave energy can be focused toward the end of the canyon by multiple reflections from the sidewalls, increasing the Froude number and causing wave breaking. Canyons can have greatly enhanced dissipation of incoming low-mode wave energy compared to planar slopes, figure2.

Impact of Distribution of Internal Tide Dissipation on Global Circulation and Climate

As a first step to refining parameterizations of the global distribution of internal wave dissipation to include the processes described above, a series of climate model "thought-experiments" were undertaken using the GFDL ESM2G model [5], in which the total energy input into the internal tide field was held constant, but the geographical distribution of the dissipation of that energy was varied [19]. Specifically, the prescription for the barotropic-to-baroclinic energy transfer [26] was employed; a fixed fraction $q_L = 20\%$ of that energy was dissipated locally, and the remainder $1 - q_L$ was distributed around the ocean in one of the following regions: i) continental slopes: all regions with slope of X; ii) deep basins: all remaining regions with depth $> 500m$; iii) continental shelves: all remaining shallow regions. The dissipation was distributed in the vertical according to three different scalings: 1) exponentially decaying away from the bottom with a fixed decay scale, as in the local component of [26]; 2) $\varepsilon \sim E \sim N$, where E is the energy density of the low-mode internal wave and N is the buoyancy frequency. This profile is suggested by full-depth overturning of the low-mode internal wave at high Froude number, e.g. for shoaling topography [14]; 3) $\varepsilon \sim E^2 \sim N^2$. This profile is suggested by observations away from topography [27] and agrees with weakly nonlinear wave-wave interaction theory. For comparison a further simulation with farfield dissipation distributed around the globe with a uniform diffusivity was carried out, similar to that used by [24].

Results show that the global ocean climate is particularly sensitive to the vertical distribution of dissipation. Dissipation higher in the water column leads to a more diffuse thermocline and enhancement of the subtropical overturning cells, higher dissipation at depth leads to enhanced deep overturning. The global circulation is less sensitive to the horizontal distribution of mixing, except where it impacts dense water formation regions. When the dense water on shelves and continental slopes which feeds the sinking branch of both north and south overturning cells is diluted before descent, the overturning is weakened. Changes to the overturning further impact the sea-surface temperature and climate [19].

Conclusions

Internal tides can break and lead to overturning and mixing when the waves have large Froude number. The internal tides predicted by linear theory at the generation site rarely satisfy this criterion for breaking, but a variety of processes can subsequently modify the Froude number. These processes include arrest of the waves by the barotropic flow at tall, steep topography; nonlinear wave-wave interactions which transfer energy to lower frequency, smaller vertical wavelength waves, and interactions with stratification, all of which can occur close to the generation site. Far from the generation site, both shoaling and focusing in canyons can increase Froude number by enhancing energy density, while topographic scattering and reflection from critical slope topography can transfer energy to very high wavenumbers. A necessary step remaining to tie together the internal wave generation and dissipation sites is a model of wave propagation, currently in progress [18].

In conclusion, many different processes cause internal tides to break at topography, both near the generation site and far away at distant continental slopes. For each of these processes, the efficiency and vertical distribution of the dissipation vary. Accurate representation of mixing due to internal tides in climate models must incorporate all these processes into a single energetically consistent framework. Climate model simulations are sensitive to the geographical distribution of the internal tide driven mixing, encouraging refinement of parameterizations which better represent the mixing due to breaking internal tides.

Acknowledgements

This paper is a review of recent work carried out in collaboration with many coauthors, in particular Jody Klymak, Maarten Buijsman, Angelique Melet, Max Nikurasin, Robert Hallberg, Young Yi, Robert Nazarian, Benjamin Mater, the participants of the ONR-funded IWISE program, and the participants in the NSF/NOAA Internal Wave Driven Mixing Climate Process Team. Any errors in this synthesis are mine alone.

References

[1] Alford, M. H., Peacock, T., MacKinnon, J. A., Nash, J. D., Buijsman, M. C., Centuroni, L. R., Chao, S.-Y., Chang, M.-H., Farmer, D. M., Fringer, O. B., Fu, K.-H., Gallacher, P. C., Graber, H. C., Helfrich, K. R., Jachec, S. M., Jackson, C. R., Klymak, J. M., Ko, D. S., Jan, S., Johnston, T. M. S., Legg, S., Lee, I.-H., Lien, R.-C., Mercier, M. J., Moum, J. N., Musgrave, R., Park, J.-H., Pickering, A. I., Pinkel, R., Rainville, L., Ramp, S. R., Rudnick, D. L., Sarkar, S., Scotti, A., Simmons, H. L., Laurent, L. C. S., Venayagamoorthy, S. K., Wang, Y.-H., Wang, J., Yang, Y. J., Paluszkiewicz, T. and Tang, T.-Y. D., The formation and fate of internal waves in the South China Sea, *Nature*, **521**, 2015, DOI:10.1038/nature14399.

[2] Bühler, O. and Holmes-Cerfon, M., Decay of an internal tide due to random topography in the ocean, *Journal of Fluid Mechanics*, **678**, 2011, 271–293.

[3] Buijsman, M., Legg, S. and Klymak, J., Double ridge internal tide interference and its effect on dissipation in Luzon Strait, *J. Phys. Oceanogr.*, **42**, 2012, 1337–1356.

[4] Carter, G. and Gregg, M., Intense, variable mixing near the head of monterey submarine canyon., *J. Phys. Oceanogr.*, **32**, 2002, 3145–3165.

[5] Dunne, J. P., John, J., Adcroft, A., Griffies, S. M., Hallberg, R. W., Shevliakova, E., Stouffer, R. J., Cooke, W. F., Dunne, K. A., Harrison, M. J., Krasting, J. P., Malyshev, S., Milly, P. C. D., Phillipps, P., Sentman, L. T., Samuels, B. L., Spelman, M. J., Winton, M., Wittenberg, A. T. and Zadeh, N., GFDL's ESM2 global coupled climate-carbon Earth System Models Part I: Physical formulation and baseline simulation characteristics, *Journal of Climate*, **25**, 2012, 6646–6665.

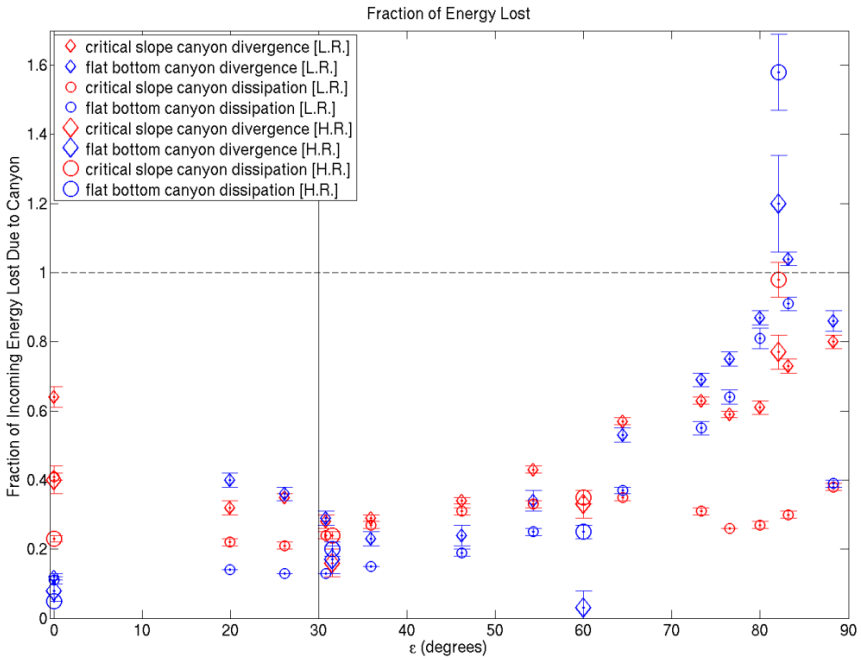

Figure 2: The fraction of incoming energy dissipated for mode-1 internal waves encountering a canyon in a continental slope, as a function of the apex angle ε of the V-shaped canyon (where 2 tan ε corresponds to the ratio of length/width, and ε increases as the canyon narrows). Symbols in blue correspond to flat bottomed canyons with vertical side walls, symbols in red correspond to a canyon with axis near the critical slope $\gamma = 1$. Large symbols correspond to high resolution simulations, small symbols to low resolution simulations. As the canyon narrows relative to its length, wave focusing increases the fraction of incoming energy which is lost to wave breaking, particularly in flat-bottomed canyons. From [20]

[6] Dunphy, M. and Lamb, K. G., Focusing and vertical mode scattering of the first mode internal tide by mesoscale eddy interaction, *J. Geophys. Res.*, **119**, 2014, 523–536.

[7] Garrett, C. and Kunze, E., Internal tide generation in the deep ocean, *Annual Review of Fluid Mechanics*, **39**, 2007, 57–87.

[8] Ivey, G. and Nokes, R., Vertical mixing due to the breaking of critical internal waves on sloping boundaries, *Journal of Fluid Mechanics*, **204**, 1989, 479–500.

[9] Ivey, G., Winters, K. and de Silva, I., Turbulent mixing in a sloping benthic boundary layer energized by internal waves, *Journal of Fluid Mechanics*, **418**, 2000, 59–76.

[10] Johnston, T. M. S., Rudnick, D. L. and Kelly, S. M., Standing internal tides in the Tasman Sea observed by gliders, *Journal of Physical Oceanography*, **45**.

[11] Klymak, J., Buijsman, M., Legg, S. and Pinkel, R., Parameterizing surface and internal tide scattering and breaking on supercritical topography: the one- and two-ridge cases, *Journal of Physical Oceanography*, **43**, 2013, 1380–1397.

[12] Klymak, J. M., Legg, S. A. and Pinkel, R., A simple parameterization of turbulent tidal mixing near supercritical topography, *Journal of Physical Oceanography*, **40**, 2010, 2059–2074.

[13] Klymak, J. M., Pinkel, R. and Rainville, L. N., Direct breaking of the internal tide near topography: Kaena Ridge, Hawaii, *Journal of Physical Oceanography*, **38**, 2008, 380–399.

[14] Legg, S., Scattering of low-mode internal waves at finite isolated topography, *Journal of Physical Oceanography*, **44**.

[15] Legg, S. and Adcroft, A., Internal wave breaking at concave and convex continental slopes, *Journal of Physical Oceanography*, **33**, 2003, 2224–2246.

[16] Legg, S. and Klymak, J. M., Internal hydraulic jumps and overturning generated by tidal flow over a steep ridge, *Journal of Physical Oceanography*, **38**, 2008, 1949–1964.

[17] MacKinnon, J. A., Alford, M. H., Sun, O., Pinkel, R., Zhao, Z. and Klymak, J., Parametric subharmonic instability of the internal tide at 29N, *Journal of Physical Oceanography*, **43**, 2013, 17–28.

[18] Mater, B., Hallberg, R., Legg, S., Adcroft, A. and Nycander, J., Representing the propagation and far-field dissipation of itnernal tides in a global climate model, *in prep*.

[19] Melet, A., Legg, S. and Hallberg, R., Climatic impacts of parameterized local and remote tidal mixing, *Journal of Climate*, **29**, 2016, doi:DOI:10.1175/JCLI–D–15–0153.1.

[20] Nazarian, R. and Legg, S., Internal wave scattering in continental slope canyons: a parameter space study, *in prep*.

[21] Nikurashin, M. and Legg, S., A mechanism for local dissipation of internal tides generated at rough topography, *Journal of Physical Oceanography*, **41**, 2011, 378–395.

[22] Polzin, K. L., An abyssal recipe, *Ocean Modelling*, **30**, 2009, 298 – 309.

[23] Polzin, K. L., Toole, J. M., Ledwell, J. R. and Schmitt, R. W., Spatial variability of turbulent mixing in the abyssal ocean, *Science*, **276**, 1997, 93–96.

[24] Simmons, H. L., Jayne, S. R., St. Laurent, L. C. and Weaver, A. J., Tidally driven mixing in a numerical model of the ocean general circulation, *Ocean Modelling*, **6**, 2004, 245 – 263.

[25] St. Laurent, L. C. and Garrett, C., The role of internal tides in mixing the deep ocean, *Journal of Physical Oceanography*, **32**, 2002, 2882–2899.

[26] St. Laurent, L. C., Simmons, H. L. and Jayne, S. R., Estimating tidally driven mixing in the deep ocean, *Geophysical Research Letters*, **29 (23)**, 2002, 2106.

[27] Waterhouse, A., MacKinnon, J. A., Pinkel, R., Simmons, H. L., Polzin, K. L., C., S. L., Sun, O., Alford, M. H., Kunze, E., Nash, J. D., Sanford, T., Lee, C., Thurnherr, A. M., Whalen, C. B. and Talley, L. D., Global patterns of diapycnal mixing from measurements of the turbulent dissipation rate, *Journal of Physical Oceanography*, **44**, 2014, 1854–1872.

[28] Yi, Y., Legg, S. and Nazarian, R., A process study of tidal mixing over rough topography, *in prep*.

[29] Zhao, Z., Alford, M. H., Girton, J. B., Rainville, L. and Simmons, H. L., Global observations of open-ocean mode-1 M_2 internal tides, *Journal of Physical Oceanography*, **46**, 2016, 1657–1684.